



ARTIFICIAL NEURAL NETWORK MODEL FOR PERFORMANCE EVALUATION OF RC RECTANGULAR BEAMS WITH EXTERNALLY BONDED GLASS FIBRE REINFORCED POLYMER REINFORCEMENT

N. Pannirselvam¹, V. Nagaradjane², K. Chandramouli³ and M. Ravindrakrishna⁴

¹VIT University, Vellore, India

²Department of Structural Engineering, Annamalai University, Annamalainagar, India

³Priyadrashini Institute of Technology for Women, Tenali, Guntur, Andhra Pradesh, India

⁴Priyadrashini Institute of Technology, Tenali, Guntur, Andhra Pradesh, India

E-Mail: npanirselvam@vit.ac.in

ABSTRACT

The effect of glass fibre reinforced polymer laminates on the performance of reinforced concrete rectangular beams having different internal steel reinforcement ratios was investigated. The parameters of investigation included yield load, ultimate load, yield deflection, ultimate deflection, maximum crack width, deflection ductility and energy ductility. Artificial Neural Network model was generated to predict the performance characteristics taking percentage of steel reinforcement, thickness of glass fibre reinforced polymer and the type of fibre used in glass fibre reinforced polymer as parameters.

Keywords: model, reinforced concrete beams, glass fibre reinforced polymer, performance evaluation, ANN, ductility, strength.

INTRODUCTION

Glass fibre reinforced polymer (GFRP) is a promising material for strengthening flexural members. The application of GFRP laminates improves the ultimate strength of reinforced concrete flexural members and results in reduced deflection when compared to the unplated specimens. The performance of GFRP plated specimens depends upon the percentage of internal steel reinforcement, properties of concrete, type of adhesive and the above all, the characteristics of the GFRP laminate. This paper presents the results of experimental investigations carried out on fifteen reinforced concrete rectangular beams along with an Artificial Neural Network (ANN) based model for performance prediction.

Flexural failure of reinforced concrete beams with externally bonded Fibre Reinforced Polymer (FRP) plates in the tension zone (Davids, W.G. *et al.*, 2004). Some of the specimens had FRP plates running the full length of the tension face and the remaining beams had FRP plates over partial length and all of them were tested under fatigue loading. The study indicated that the fatigue resistance of beams with full-length and partial plating proved to perform adequately under fatigue load while the unplated specimens performed very poorly.

Lee H.K. and Hausmann L.R. (2004) have studied on structural repair and strengthening of damaged RC beams with Sprayed FRP (SFRP). Ultimate load capacity, ductility and energy absorption were studied in the context of coating thickness, fibre length, fibre loading and type of fibre. The study concluded that SFRP is capable of substantially increasing the load capacity, ductility and energy absorbing capacity.

Ascione *et al.*, (2005) studied the behaviour of reinforced concrete T-Beam fitted with mechanically fastened FRP plate on the soffit. Ratio between length of the external plate to the length of the strengthened beam, mechanical properties of the composite plate, properties of

the adhesive at the interface between the concrete surface and the FRP plate were the parameters studied. The investigation found that the ratio between the peak value and mean value of longitudinal shear increases with decrease in plate length and the thickness of the adhesive layer and increase in stiffness of the FRP plate and of the adhesive. The evaluation of the peak value of the longitudinal shear interactions is of important to prevent premature failure of plated beams.

RESEARCH SIGNIFICANCE

The present research investigation is aimed at studying the increase in moment carrying capacity obtained by the application of GFRP laminates of two types: i) Chopped Strand Mat (CSM) and ii) Woven Rovings (WR) on reinforced concrete rectangular beams having internal tensile steel ratios of 0.4%, 0.6% and 0.9%. The effect of thickness GFRP, type of fibre used in GFRP and percentage tensile steel reinforcement on the yield load, ultimate load, yield deflection, ultimate deflection, maximum crack width, deflection ductility and energy ductility was investigated by applying 3 mm and 5 mm laminates. The results obtained from the investigation were used to generate an ANN based design tool for estimating the thickness of laminate required to achieve a desired ultimate moment carrying capacity for a rectangular beam with known steel ratio. The design tool is aimed to serve the field engineers and academicians to help estimate the amount of FRP material to be applied on the soffit of rectangular beam.

SPECIMEN DETAILS

Reinforced concrete rectangular beam specimens with 250×150×3000 mm were cast. Tensile steel reinforcement was provided at 0.4% (2 bars, 10 mm dia.), 0.6% (2 bars, 12 mm dia.) and 0.9% (3 bars 12 mm dia.). The reinforcement details are shown in Figure-1. Five



specimens were cast for each series; one of them was used as reference specimen and tested without any laminate while four others were plated with 3 mm and 5 mm thick GFRP laminates containing CSM and WR fibres. Table-1

shows the details of the fifteen specimens used for testing. Shear stirrups and reinforcement were adequately designed to resist abnormal modes of failure in shear or failure in flange portion.

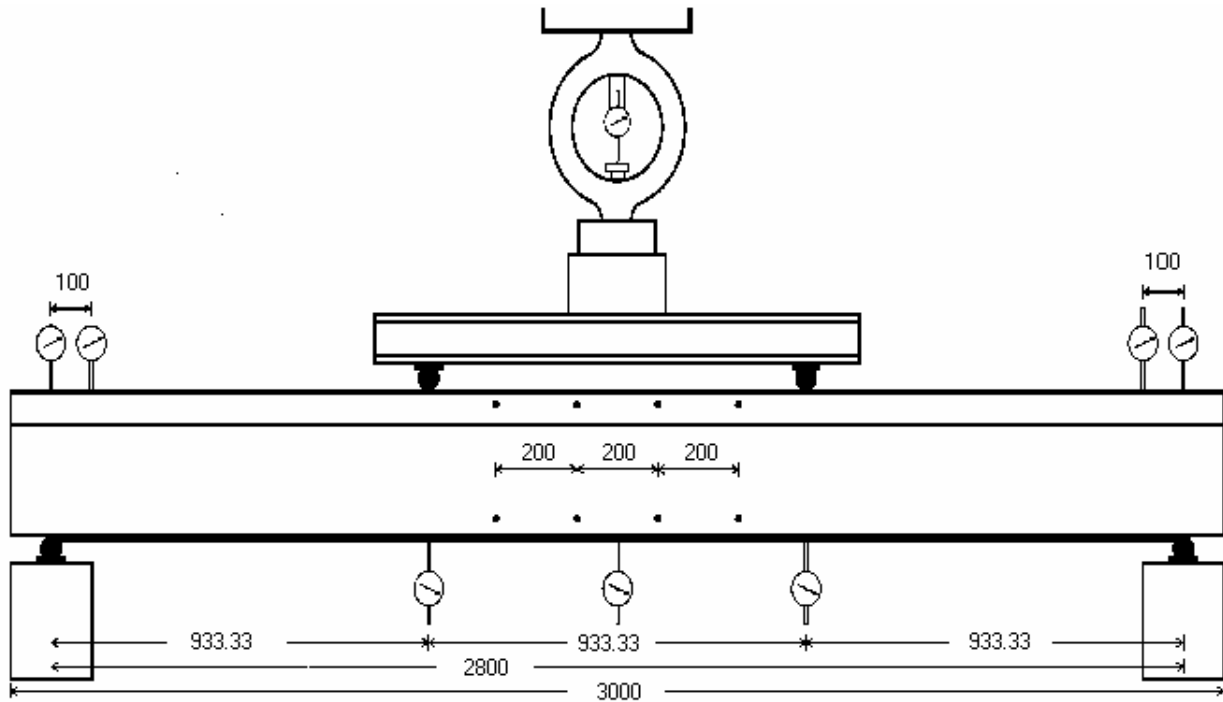


Figure-1. Details of test beam.

Table-1. Specimen details.

S. No.	Beam designation	% Steel reinforcement	Type of GFRP	Thickness of GFRP	Composite ratio (area of FRP / area of steel)
1.	SR1	0.419	-	-	-
2.	SR1CSM3	0.419	CSM	3	2.387
3.	SR1CSM5	0.419	CSM	5	3.979
4.	SR1WR3	0.419	WR	3	2.387
5.	SR1WR5	0.419	WR	5	3.979
6.	SR2	0.603	-	-	-
7.	SR2CSM3	0.603	CSM	3	1.562
8.	SR2CSM5	0.603	CSM	5	2.653
9.	SR2WR3	0.603	WR	3	1.592
10.	SR2WR5	0.603	WR	5	2.653
11.	SR3	0.905	-	-	-
12.	SR3CSM3	0.905	CSM	3	1.231
13.	SR3CSM5	0.905	CSM	5	2.051
14.	SR3WR3	0.905	WR	3	1.231
15.	SR3WR5	0.905	WR	5	2.051

Note: CSM - chopped strand mat; WR - woven rov



MATERIAL PROPERTIES

Cement concrete having compressive strength 28.54 MPa and elasticity modulus 24.20 GPa was used for casting the specimens. Steel reinforcement was provided with Fe 415 grade steel rods having yield strength of 415 MPa as main reinforcement. 2 legged 8 mm dia. rolled tar steel rods were used for shear reinforcement at 100 mm c/c in order to avoid premature failure of specimen in shear. The tensile strength and percentage elongation at ultimate load for CSM and WR fibre reinforced GFRP laminates were determined in accordance with ASTM 638.

Table-2 shows the properties of GFRP materials used in the experimental work.

Two part epoxy adhesive with ground silica powder filler was used for bonding the GFRP laminates to the soffit of the beam. Thickness of adhesive was maintained at 2 mm over the entire soffit portion. The properties of epoxy adhesive are presented in Table-3. The adhesive was a proprietary formulation and supplied in the form of Compound - A, Compound - B and ground silica powder, to be mixed in the ratio of 2:1:1 in the respective order.

Table-2. Properties of GFRP laminates.

S. No.	Type of fibre in GFRP	Thickness (mm)	Tensile strength (MPa)	Ultimate elongation (%)	Elasticity modulus (MPa)
1	CSM	3	126.2	1.69	7467.46
2	CSM	5	156	1.37	11386.86
3	WR	3	147.4	2.15	6855.81
4	WR	5	163.5	2.01	8134.33

Table-3. Properties of epoxy adhesive.

S. No.	Property	Test value (In accordance with ASTM 638)
1	Tensile strength at break (MPa)	2.80
2	Elongation at break (%)	16.00
3	Elasticity modulus (MPa)	14.60
4	Tensile strength at Yield (MPa)	3.50
5	Shear strength (MPa)	6.00
6	Flexural strength (MPa)	0.32
7	Compressive strength (MPa)	10.5

SPECIMEN PREPARATION AND TESTING

The specimen were prepared for GFRP lamination by applying wire brush followed by grinding stone to remove all loose material on the soffit portion and to ensure adequate adhesion. Epoxy adhesive was prepared by mixing compound - A and compound - B along with ground silica powder. The adhesive was spread as a uniform layer on the soffit of the beams, with thickness not less than 2 mm. The GFRP laminate is applied to the soffit of beam by gently pressing the sheet from one end of the beam to the other along the length of beam.



Figure-2. Test setup and instrumentation.

All the beams were tested under four point bending on loading frame of 50 T capacity. Instrumentation included the dial gauges at the soffit, one below the left support, one at the midspan and the third



below the right load. The beams had 100 mm bearing on both ends, resulting in a span of 2800 mm. Two point loads were applied at middle third points of the span. One support was placed on roller end and the other was placed on a hinge. Two dial gauges each were mounted on the compression face of the specimen over both supports to measure slope at both ends. For this purpose, one dial gauge was placed exactly over the support and the other at a distance of 100 mm from the support, over each support. The slope can be estimated using the relation,

$$\theta_{\text{sup port}} = \frac{\Delta_i - \Delta_s}{\Delta_x} \quad (1)$$

Where, $\theta_{\text{sup port}}$ is the slope over the support, Δ_i and Δ_s are the deflections found from the dial gauges located 100 mm away from the support and exactly over the support respectively, Δ_x is the distance between the dial gauges, which is 100 mm in the present study.

Ultimate deflection of the beam was measured with a help of a large metallic dial whose pointer was attached to a small spindle. A thread was taken around the spindle, with one end tied to the mid span point, the other end being weighed adequately to ensure rotation of the spindle without any slackening. This arrangement permitted measurement of deflection up to ultimate load levels, since the dial can remain in place without any damage under the beam. Digital Demountable Mechanical Extensometers (DEMEC) gauges were used to measure the amount of contraction in compression zone and extension in tension zone of the beam.

TEST RESULTS AND DISCUSSIONS

The experimental results are summarized in Tables 4 to 6. The results indicate that that the presence of GFRP laminates leads to increase in first crack load, yield load and ultimate load. For specimens with 3 mm thick laminates, the percentage increase in first crack load is more than those for yield load and ultimate load. For specimens bonded with 5 mm thick laminates, the percentage increase in ultimate load carrying capacity is higher than or commensurate with the percentage increase in first crack load. This indicates that the linear elastic behaviour of beams is ensured more in the case of low thickness laminates than in the case of high thickness laminates. Studies with more variations in thickness would be needed confirm the trend identified here.

It is noted that some of the specimens seem to show decrease in yield load capacity and the decrease is in

the range of 4.13% to 19.42%. This might be attributed to the fact that the actual yield point was located somewhere between the yield load identified and the next load increment applied on the frame. Ultimate load carrying capacity increases with increase in GFRP laminate thickness. Ultimate deflection of GFRP plated beams shows considerable reduction. Reduction in crack width shows positive trend with increasing GFRP laminate thickness. More the thickness of GFRP laminates more the reduction in crack width.

Ductility is calculated based on deflection and energy approaches and the ratio of ductility between the GFRP plated specimens and reference specimen is calculated. Deflection ductility is calculated using the expression,

$$\eta_d = \frac{\Delta_{ult}}{\Delta_{yield}} \quad (2)$$

Where η_d is the deflection ductility, Δ_{ult} and Δ_{yield} are the ultimate and yield deflections respectively. Energy ductility is calculated using,

$$\eta_e = \frac{\sum_{i=1}^{N_{ult}-1} \frac{(P_i + P_{i+1})(\Delta_{i+1} - \Delta_i)}{2}}{\sum_{i=1}^{N_{yield}-1} \frac{(P_i + P_{i+1})(\Delta_{i+1} - \Delta_i)}{2}} \quad (3)$$

where, η_e is the energy ductility, N_{ult} is the index number of ultimate load step, N_{yield} is the index number of yield load, P_i is the load at i^{th} step, P_{i+1} is the load at step next to the the i^{th} step, Δ_i is the load at i^{th} step and Δ_{i+1} is the deflection at step next to the the i^{th} step. Table-6 indicates that there is increase in ductility for beams plated with GFRP laminates and that the level of apparent increase is more using the energy approach than the deflection approach. This is indicative of the the fact that the failure mode essentially becomes brittle in for GFRP plated beams, since more energy is absorbed by increase in load carrying capacity than increase in deflection capacity.

**Table-4.** Strength of GFRP plated RC beams.

#	Beam specification	First crack load (kN)	Increase in first crack load (%)	Yield load (kN)	Increase in yield load (%)	Ultimate load (kN)	Increase in ultimate load (%)
1	SR1	17.17	0.00	17.17	0.00	34.34	0.00
2	SR1CSM3	17.17	0.00	22.07	28.54	36.79	7.13
3	SR1CSM5	24.53	42.87	39.24	128.54	49.05	42.84
4	SR1WR3	17.17	71.40	44.15	157.13	58.86	71.40
5	SR1WR5	26.98	100.00	51.5	199.94	63.77	85.70
6	SR2	22.07	0.00	34.34	0.00	41.69	0.00
7	SR2CSM3	24.53	57.13	41.69	21.40	53.96	29.43
8	SR2CSM5	24.53	42.87	44.15	28.57	61.31	47.06
9	SR2WR3	46.60	114.27	49.05	42.84	73.58	76.49
10	SR2WR5	29.43	185.67	56.41	64.27	88.29	111.78
11	SR3	36.79	0.00	36.79	0.00	63.77	0.00
12	SR3CSM3	41.69	-10.03	51.5	39.98	66.22	3.84
13	SR3CSM5	34.34	89.97	58.86	59.99	80.93	26.91
14	SR3WR3	49.05	69.96	74.8	103.32	78.48	23.07
15	SR3WR5	53.96	119.98	58.86	59.99	105.46	65.38

Table-5. Deformation and crack width of GFRP plated RC beams.

#	Beam specification	Deflection at first crack (mm)	Change in deflection at first crack load (%)	Deflection at yield load (mm)	Change in deflection at yield load (%)	Ultimate deflection (mm)	Change in ultimate deflection (%)	Crack width at ultimate load (mm)	Change in crack width at ultimate load (%)
1	SR1	4.52	0.00	11.17	0.00	30.2	0.00	1.20	0.00
2	SR1CSM3	3.38	-25.22	8.04	-28.02	32.73	8.38	1.00	-16.67
3	SR1CSM5	6.55	44.91	8.44	-24.44	35.6	17.88	0.60	-50.00
4	SR1WR3	7.77	71.90	11.58	3.67	32.83	8.71	0.82	-31.67
5	SR1WR5	7.39	63.50	7.98	-28.56	35.49	17.52	0.62	-48.33
6	SR2	3.29	0.00	10.91	0.00	33.7	0.00	1.04	0.00
7	SR2CSM3	5.09	54.71	9.64	-11.64	33.82	0.36	0.64	-38.46
8	SR2CSM5	3.89	18.24	8.43	-22.73	37.15	10.24	0.52	-50.00
9	SR2WR3	6.32	92.10	9.85	-9.72	35.05	4.01	0.66	-36.54
10	SR2WR5	11.72	256.23	10.63	-2.57	44.38	31.69	0.58	-44.23
11	SR3	3.75	0.00	10.4	0.00	33.89	0.00	0.90	0.00
12	SR3CSM3	4.52	20.53	9.57	-7.98	35.05	3.42	0.40	-55.56
13	SR3CSM5	7.51	100.27	9.11	-12.40	38.68	14.13	0.54	-40.00
14	SR3WR3	7.47	99.20	9.86	-5.19	37.52	10.71	0.54	-40.00
15	SR3WR5	9.2	145.33	9.2	-11.54	45.64	34.67	0.52	-42.22



Table-6. Ductility of GFRP plated RC beams.

#	Beam specification	Deflection ductility	Deflection ductility ratio	Energy ductility	Energy ductility ratio
1	SR1	2.7	3.83	1	1
2	SR1CSM3	4.07	6.64	1.51	1.73
3	SR1CSM5	4.22	8.29	1.56	2.17
4	SR1WR3	2.84	4.94	1.05	1.29
5	SR1WR5	4.45	8.05	1.64	2.1
6	SR2	3.09	4.77	1	1
7	SR2CSM3	3.51	6.27	1.14	1.31
8	SR2CSM5	4.41	8.02	1.43	1.68
9	SR2WR3	3.56	6.38	1.15	1.34
10	SR2WR5	4.17	9.33	1.35	1.95
11	SR3	3.26	5.82	1	1
12	SR3CSM3	3.66	8.08	1.12	1.39
13	SR3CSM5	4.25	8.82	1.3	1.51
14	SR3WR3	3.81	8.07	1.17	1.39
15	SR3WR5	4.96	14.06	1.52	2.42

GENERAL REGRESSION NEURAL NETWORK (GRNN) MODELING TOOL

The GRNN is a fixed topology network, where the number of layers is fixed. It contains two layers for

processing the input data. But, the number of neurons in each layer would differ based on the data provided at the time of initialization. The architecture of GRNN is shown in Figure-3.

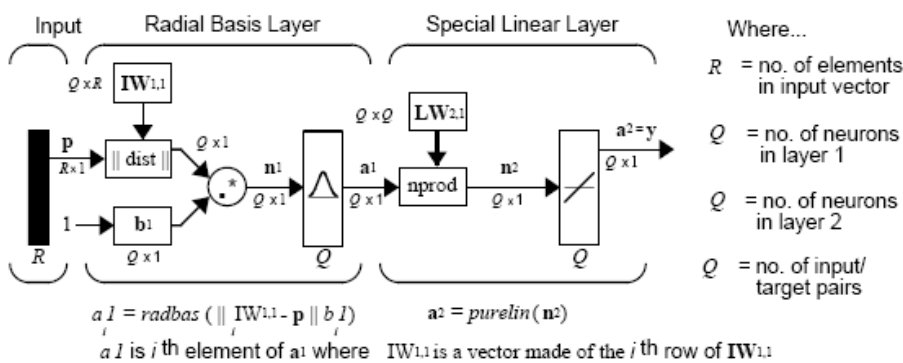


Figure-3. Architecture of GRNN.

DEVELOPING ANN BASED PERFORMANCE PREDICTION TOOL

ANN requires generation of object for each parameter taken up for prediction. Prediction system is developed for yield load, ultimate load, yield deflection, ultimate deflection, crack width at ultimate load,

deflection ductility, energy ductility, deflection ductility ratio and energy ductility ratio. The inference systems take percentage of steel reinforcement, type of GFRP and thickness of GFRP laminate as input parameters.

The inference systems were generated on MATLAB software using GRNN toolbox. The generation



of the model was a two step process, the first step being creation of a GRNN. After generating individual inference system objects for each prediction parameter, all the objects are saved into disk file, in order to make them available for client programs. The coding for the above work was developed in a script file. A graphical user interface was also developed to take visual input from the user, reading the appropriate from disk file and displaying predicted values. Figures 4 to 9 show selective screen shots. The performance of the inference systems was measured using Root Mean Square Error (RMSE) and the values are presented in Table-7.

Table-7. Performance of GRNN model.

#	Parameter	RMS error
1.	Yield load (kN)	7.32
2.	Ultimate load (kN)	10.20
3.	Yield deflection (mm)	0.48
4.	Ultimate deflection (mm)	0.88
5.	Maximum crack width (mm)	0.11
6.	Deflection ductility	0.22
7.	Energy ductility	0.51
8.	Deflection ductility ratio	0.12
9.	Energy ductility ratio	0.19

CONCLUSIONS

Application of GFRP laminates leads to increase in load carrying capacity to the extent of 63.77% over the unplated reference specimens. Increase in steel ratio was found to decrease the effectiveness of the externally bonded GFRP laminates with respect to increase in ultimate load and deflection ductility. WR of 3 mm and 5 mm thickness performed better than their CSM counterparts for all steel ratios. The reference specimens having 0.4%, 0.6% and 0.9% steel reinforcement showed consistent increase in load carrying capacity. The reduction in ultimate deflection was upto the extent of 0.30% for 3 mm CSM plated specimens and 10.24% for 5 mm thick CSM plated specimens. The reduction in maximum crack width was up to 40.00 and 55.56% for 3 mm and 5 mm CSM plated specimens. Crack width reduction due to the application of GFRP laminates was more for higher steel ratios.

ANN based model provided reasonable prediction system to estimate the first crack load, yield load, ultimate load, deflection at first crack load, deflection at yield load, deflection at ultimate load, maximum crack width, deflection ductility and energy ductility for GFRP plated reinforced concrete beams, for known thickness of GFRP, steel ratio and type of GFRP.

The RMS error values associated with the model indicate that the predicted results are in good agreement with experimental results.

REFERENCES

ACI Committee 318. 1999. Building Code Requirements for Structural Concrete and Commentary. American Concrete Institute, Farmington Hills, Michigan, USA.

ACI Committee 440.2R-02. 2002. Guide for the Design and Construction of Externally Bonded FRP Systems for Strengthening Concrete Structures. American Concrete Institute, Farmington Hills, Michigan, USA.

Ahmed Khalifa, William J. Gold Antonio Nanni and Abdel Aziz, M.I. 1998. Contribution of Externally Bonded FRP to Shear Capacity of Flexural Members. *Journal of Composites for Construction*, ASCE. 2(4): 195- 203.

Ascione L., Berardi V.P., Feo L. and Mancusi G. 2005. A numerical evaluation of the interlamionar stress state in externally FRP plated RC beams. *Journal of Composites*. 36(B):0 83-90.

Barros J.A.O. and Fortes A.S. 2005. Flexural strengthening of concrete beams with CFRP laminates bonded into slits. *Journal of Cement and Concrete Composites*. 27: 471-480.

Campione G. 2006. Influence of FRP Wrapping techniques on the compressive behaviour of concrete prisms. *Journal of Cement and Concrete Composites*. 28(5): 497-505.

Coronado C.A and Lopez M.M. 2006. Sensitivity Analysis of Reinforced Concrete Beams Strengthened with FRP Laminates. *Journal of Cement and Concrete Composites*. pp. 102-114.

Dubois D. and Prade H. 1980. *Fuzzy Sets and Systems: Theory and Applications*. Academic Press, New York.

Gao B., Leung C.K.Y. and Kim J.K. 2005. Prediction of Concrete Cover Separation Failure for RC Beams Strengthened with CFRP Strips. *Journal of Engineering Structures*. 27: 177-189.

Hamoush S.A. and Ahmad S.H. 1990. Debonding of Steel Plate-Strengthened Concrete Beams. *Journal of Structural Engineering*, ASCE. 116(2): 356-371.

Liu I., Oehlers D.J., Seracino R. and Ju G. 2006. Moment Redistribution Parametric Study of CFRP, GFRP and Steel Surface Plated RC Beams and Slabs. *Journal of Construction and Building Materials*. 20(1): 59-70.

The MathWorks. 2002. *Fuzzy Logic Toolbox for Use with MATLAB®*, User's Guide (version 2.1.2).

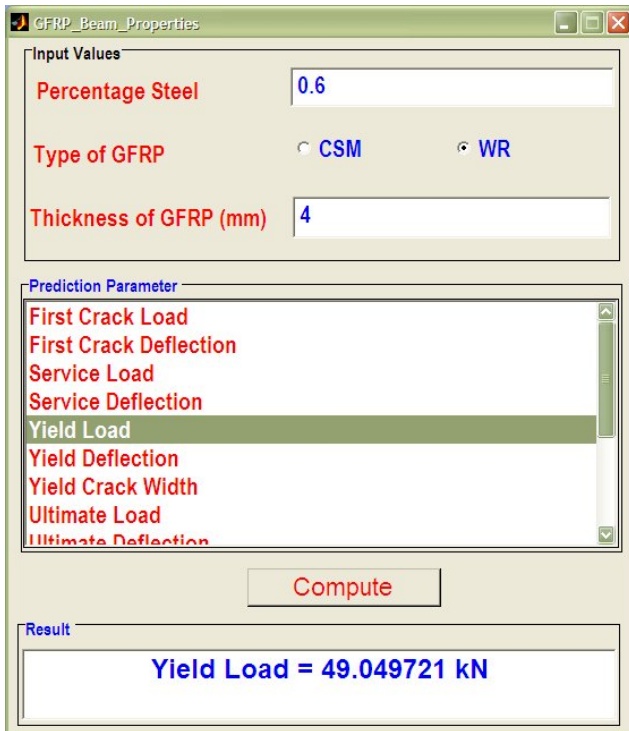


Figure-4. Prediction of yield load from GUI.

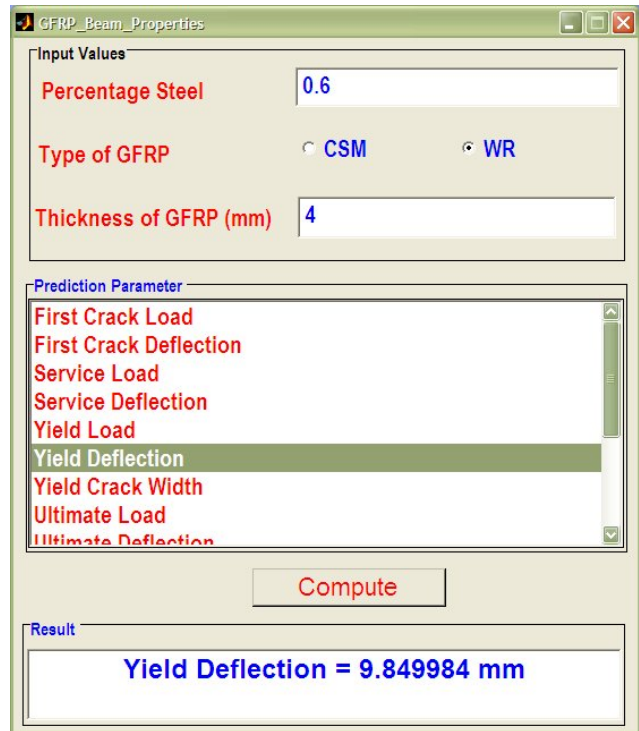


Figure-6. Prediction of yield deflection from GUI.

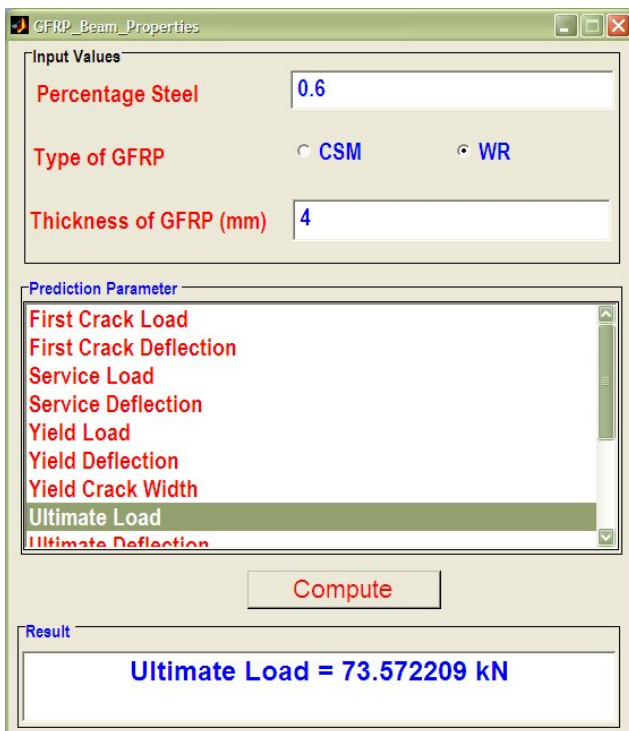


Figure-5. Prediction of ultimate load from GUI.

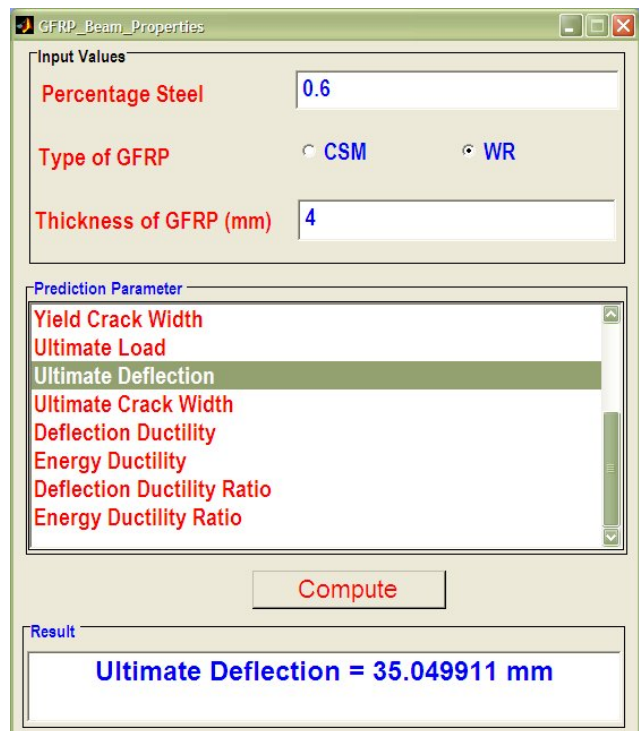


Figure-7. Prediction of ultimate deflection from GUI.



The screenshot shows the 'GFRP_Beam_Properties' software interface. Under 'Input Values', 'Percentage Steel' is 0.6, 'Type of GFRP' is WR (selected), and 'Thickness of GFRP (mm)' is 4. The 'Prediction Parameter' list includes Yield Crack Width, Ultimate Load, Ultimate Deflection, Ultimate Crack Width, Deflection Ductility, Energy Ductility, Deflection Ductility Ratio, and Energy Ductility Ratio. The 'Compute' button is visible. The 'Result' section displays 'Energy Ductility Ratio = 1.336118'.

Figure-8. Prediction of energy ductility.

The screenshot shows the 'GFRP_Beam_Properties' software interface with the same input values as Figure 8. In the 'Prediction Parameter' list, 'Deflection Ductility Ratio' is highlighted. The 'Compute' button is visible. The 'Result' section displays 'Deflection Ductility Ratio = 1.152029'.

Figure-9. Prediction of deflection ductility.